

The aromatic hydrocarbon resins with various hydrogenation degrees Part 1. The phase behavior and miscibility with polybutadiene and with polystyrene

Jin Kon Kim*, Du Yeol Ryu, Kyung-Hee Lee

*Department of Chemical Engineering and Polymer Research Institute, Electric and Computer Engineering Division,
Pohang University of Science and Technology, Pohang, Kyungbuk 790-784, Korea*

Received 20 April 1999; received in revised form 30 July 1999; accepted 9 August 1999

Abstract

The miscibility of hydrogenated aromatic hydrocarbon resin (HR) with polybutadiene (PB) and polystyrene (PS) was investigated using turbidity measurement. Hereafter, the aromatic hydrocarbon resin having nine carbon atoms per monomer is referred to as C-9 resin. We found that C-9 resin, which has only a limited (or partial) miscibility with PB, became completely miscible with PB as the degree of hydrogenation (DH) in HR was increased to the optimum value of DH. The hydrogenation reaction of C-9 resin, which was conducted in the presence of a palladium (Pd) catalyst supported by activated carbon, converted aromatic rings in the resin to alicyclic rings. We controlled DH of C-9 resin by monitoring the amount of hydrogen used and the duration of reaction. The DH in HR was determined by elemental analysis and density measurement, and the chemical structures of HRs were determined by Fourier transform infrared spectroscopy, ^1H and ^{13}C nuclear magnetic resonance spectroscopy, and ultraviolet/visible light spectroscopy. On the basis of the results of the upper critical solution temperatures of the blend systems investigated, it was found that a favorable interaction between PS and HRs decreased steadily with increasing DH and that there exists an optimum value of DH (approximately 0.7) in HR that gives the most favorable interaction with PB. The significance of the enhanced miscibility between PB and HRs, compared to the miscibility between PB and C-9 resin, was demonstrated by measuring the tack property of pressure-sensitive adhesives (PSAs), which were prepared from a polystyrene-*block*-polybutadiene-*block*-polystyrene (SBS triblock) copolymer and HRs, and from an SBS triblock copolymer and neat C-9 resin. We found that the probe tack of SBS triblock copolymer/HRs mixtures goes through a maximum (1100 g/cm²) for HR having DH = 0.7, at which HR has the most favorable interaction with PB as determined from turbidity measurement, whereas the probe tack of SBS triblock copolymer/C-9 resin mixture is negligibly small. These results were qualitatively interpreted by the solubility parameter approach using group contribution method. © 2000 Elsevier Science Ltd. All rights reserved.

Keywords: C-9 resin; Hydrogenation; Miscibility

1. Introduction

Various kinds of elastomers have been used for pressure-sensitive adhesives (PSAs) and hot-melt adhesives. However, elastomers alone cannot provide desired properties, such as peel strength, tack properties and holding power. Thus, low-molecular-weight hydrocarbon resins, for instance, aliphatic C-5 resins, aromatic C-9 resins, hydrogenated derivatives of C-5 and C-9 resins, and rosin derivatives, are added to an elastomer in order to improve the wettability and the contact strength on the surface. Here, C-5 and C-9 resins represent the aliphatic hydrocarbon resin

having five carbon atoms per monomer, and the aromatic hydrocarbon resin having nine carbon atoms per monomer, respectively. These resins are commonly referred to as ‘tackifying resins’, which have molecular weights ranging from 300 to 3000 and usually exhibit a glassy state at room temperature [1]. Thus, PSAs consist of an elastomer and a tackifying resin.

The literature suggests that not only viscoelastic properties, but miscibility of the constituent components of a PSA plays an important role in the formulation of PSAs. Aubrey and Sherriff [2] correlated the viscoelasticity of PSA to peel adhesion strength. Sherriff et al. [3,4] reported that the addition of a tackifying resin to an elastomer shifted the onset of the transition zone to a lower frequency and also reduced the plateau modulus. Using polystyrene-*block*-polyisoprene-*block*-polystyrene (SIS triblock) copolymers

*Corresponding author. Tel.: +82-562-279-2276; fax: +82-562-279-8298.

E-mail address: jkkim@postech.ac.kr (J.K. Kim).

blended with mid-block associating resins, Kraus and coworkers [5–8] showed that the glass transition temperature (T_g) of polyisoprene (PI) mid-block increased and the plateau modulus decreased with increasing amount of tackifying resins. Class and Chu [9] carried out an extensive study on the effect of chemical structure (e.g., aromatic; aliphatic; alkyl-aromatic), the amount and molecular weight of tackifying resins on the dynamic mechanical properties of the blends composed of natural rubber or polystyrene-*ran*-polybutadiene and tackifying resins. They found that the experimentally determined T_g of the blend was consistent with the prediction by the Fox equation [10]. Han et al. [11–13] reported that the order–disorder transition temperature (T_{ODT}) of a mixture composed of an SIS triblock copolymer or polystyrene-*block*-polybutadiene-*block*-polystyrene (SBS triblock) copolymer and a tackifying resin varied with the chemical structure and the molecular weight of the resin. They reported that increasing the amount of tackifying resin decreased the T_{ODT} of the mixture when a low-molecular-weight resin was associated with the PI or polybutadiene (PB) mid-block, while the T_{ODT} of the mixture increased when the tackifying resin was associated with the polystyrene (PS) block.

According to the Dahlquist criterion [14], the plateau modulus ($G_{N,b}^0$) of PSAs consisting of a block copolymer and a tackifying resin should be less than approximately 3×10^5 Pa in order to exhibit good tack properties. In the PSA industry it is well accepted today that PSAs composed of an SIS triblock copolymer and a low-molecular-weight hydrocarbon resin have much better tack properties than PSAs composed of an SBS triblock copolymer and the same hydrocarbon resin [15]. This is attributable, at least in part, to the difference in plateau modulus between PB and PI. It is reported [16] that for low vinyl contents in PB and PI, the plateau modulus of PB ($G_{N,PB}^0$) is 1.15×10^6 Pa and that of PI ($G_{N,PI}^0$) is 3.5×10^5 Pa, i.e. ($G_{N,PB}^0$) $\approx 3G_{N,PI}^0$. Note that the values of $G_{N,PB}^0$ and $G_{N,PI}^0$, respectively, depend on the microstructures of the polymers [16]. One can estimate $G_{N,b}^0$ from $G_{N,b}^0 = \phi_{\text{block}}^\alpha G_{N,i}^0$ ($i = \text{PB or PI}$), where ϕ_{block} is the volume fraction of block copolymer in a mixture consisting of a block copolymer and a tackifying resin, and α is a scaling constant having a value between 2 and 2.25 [17].

It has been known for some time that when aromatic C-9 resin is mixed with an SBS triblock copolymer to formulate a PSA, the mixture does not provide good tack properties. This is believed to be due to only a limited miscibility between the two components. In order to overcome this shortcoming, the PSA industry has recently introduced hydrogenated C-9 resins (HRs). We expect intuitively that a favorable interaction between HRs and SBS triblock copolymer would be larger than that between C-9 resin and SBS triblock copolymer. This is because hydrogenation of aromatic C-9 resin gives rise to alicyclic compounds, which certainly would exhibit more favorable interaction with the PB block of SBS triblock copolymer than with the aromatic

C-9 resin. Here, the degree of hydrogenation (DH) represents the conversion of the aromatic rings to the alicyclic rings in a C-9 resin. Interestingly, however, the tack properties of the mixtures of SBS triblock copolymer and HRs with DH greater than 0.8 were found to be rather poor. In order to understand this seemingly peculiar behavior, one must have HRs with varying DHs. Further, the miscibility between PS and C-9 resin, and between PS and HRs, must be investigated because most commercially available SBS triblock copolymers (e.g., Kraton D series) have about 18–40 wt% of PS block.

During the past decade, many researchers have studied the miscibility of polymer blends in which one of the constituent components is fully hydrogenated. In investigating the miscibility of the blend of poly(1,2-butadiene-*co*-1,4-butadiene) and hydrogenated terpene tackifying resins, Akiyama and coworkers [18–20] observed the most favorable interaction when the mole fraction of 1,2-PB in the copolymer was about 0.5. Also, Han and coworkers [21] investigated the phase behavior of PS/PB and PS/hydrogenated PB (poly(ethylene-*co*-butene-1):PEB) blends. They found that the miscibility of the blends depended greatly on the amount of 1,2-addition in PB or PEB. However, to the best of our knowledge, no study has ever been reported on the effect of the DH of aromatic C-9 resin on the miscibility of polymer blends.

Very recently, we investigated, via turbidity measurement, the miscibility of: (i) mixtures of PB and C-9 resin with and without hydrogenation; and (ii) mixtures of PS and C-9 resin with and without hydrogenation. For the study the degree of hydrogenation of C-9 resin was varied by controlling the amount of hydrogen used and the duration of reaction. On the basis of the phase behavior of the mixtures, the Flory–Huggins interaction parameters were determined. It was found that the miscibility of the mixtures depended greatly on the DH of C-9 resin, and the most favorable interaction (or the smallest Flory interaction parameter χ) was observed when the DH was ca. 0.7. In this paper, we report the highlights of our findings.

2. Experimental section

2.1. Materials

A polybutadiene and two polystyrenes (PS-8 and PS-200) were prepared by anionic polymerization in cyclohexane with *sec*-BuLi as an initiator. The weight average molecular weight (\bar{M}_w) was determined using low-angle laser-light scattering and the molecular weight distribution (\bar{M}_w/\bar{M}_n) was determined using gel permeation chromatography (GPC, Waters Company). The microstructures of the PB were determined by ^1H and ^{13}C nuclear magnetic resonance spectroscopy (NMR, Bruker DRX500). The content of the 1,2-addition in the PB was found to be 10.0 mol%, which is almost identical to that in the PB block of the SBS triblock

Table 1
The molecular characteristics of polystyrenes and polybutadiene

Sample code	\bar{M}_w	\bar{M}_w/\bar{M}_n^a	Microstructure (mol%) ^b		
			1,2	<i>trans</i> -1,4	<i>cis</i> -1,4
PS-200	197 500 ^a	1.07	–	–	–
PS-8	7600 ^a	1.07	–	–	–
PB	676 000 ^c	1.07	10.0	48.8	41.2

^a Determined by GPC measurement.

^b Determined by a ¹H NMR spectrometer.

^c Determined by a low-angle laser light scattering (LALLS) device.

copolymers commercially available (e.g., Kraton D1102). The (\bar{M}_w) and (\bar{M}_w/\bar{M}_n) of the two PSs were determined by GPC based on PS standards. The molecular characteristics of the PB and two PSs synthesized are summarized in Table 1.

The C-9 resin synthesized by cationic polymerization with AlCl₃ as an initiator was kindly supplied by the Kolon Petrochemical Company in Korea. From the information received from the resin supplier, C-9 resin is a

copolymer consisting of vinyl toluene and indene monomers. The chemical structure of C-9 resin was investigated by ¹H NMR operating at 500 MHz and ¹³C NMR spectroscopy (Bruker DRX500) and given in Fig. 1(a) and (b), respectively. From Fig. 1(a), one notes that the peak at 7.2 ppm corresponds to aromatic hydrogen, and the peaks at 0.4–3.4 ppm correspond to the aliphatic hydrogen in the resin. From the ratio of the peak area located at 2.5–3.1 ppm, corresponding to the hydrogen of methylene (CH₂) in a five-membered ring in the indene unit, to the peak area located at 2.1–2.5 ppm, corresponding to the hydrogen of methyl (CH₃) attached to a vinyl toluene unit, the mole ratio of indene unit to vinyl toluene unit in neat C-9 resin was estimated to be one to one. Although the peak at 2.3 ppm looks a single peak, it was found that this peak is a mixture of three peaks at 2.32, 2.29 and 2.23 ppm, respectively (marked by the arrows; see inside peaks in the inset of Fig. 6). These three peaks correspond to the hydrogen of the methyl group in *ortho*, *meta* and *para* isomers of the vinyl toluene. From the peak deconvolution, we consider that among the three isomers the mole fraction of the *ortho* isomer was the largest, followed by the *meta* isomer, with the *para* isomer being the least.

It is also seen from Fig. 1(b) that (i) the peaks at 120–151 ppm correspond to the aromatic carbons (a–d); (ii) the peaks at 38–52 ppm to the main chain carbon (e); (iii) the peak at 31 ppm to the methylene bridge carbon (f) in the indene; (iv) the peaks at 18–22 ppm to the methyl carbon (g) attached benzene ring of vinyl toluene; and the peak at 15 ppm to the methyl end carbon (h). From the peaks corresponding to carbons (a), (c) and (g), vinyl toluene has three isomers, *ortho*, *meta* and *para* isomers. Finally, \bar{M}_w and \bar{M}_w/\bar{M}_n of the C-9 resin, determined by GPC (based on PS standards), were found to be 1000 and 1.45, respectively.

2.2. Hydrogenation reaction

The double bonds in the aromatic rings (vinyl toluene and indene units) of C-9 resin (Fig. 2(a)) were saturated (or hydrogenated), yielding alicyclic rings, using a parr reactor with the capacity of 300 ml. The solvent was cyclohexane (polymer concentration was 150 g/l), and the catalyst employed in this study was palladium (Pd) supported by activated carbon (10 wt% Pd, Aldrich Company). Previously, Gelsen and Bates [22,23] reported that in the presence of Pd catalyst, the benzene ring in PS was fully hydrogenated, yielding poly(vinyl cyclohexane) (PVCH). The concentration of catalyst was 0.15 g per 1 g of C-9 resin. The hydrogenation reaction employed in the present study was as follows. First, the parr reactor containing the polymer solution (ca. 160 ml) in cyclohexane in the presence of the catalyst was purged by fresh hydrogen gas (purity over 99.999%) for 4–5 min at room temperature; then reactor pressure was increased to 10 bar without stirring. Next, while stirring the solution vigorously (ca. 2000 rpm), we increased the reaction temperature slowly

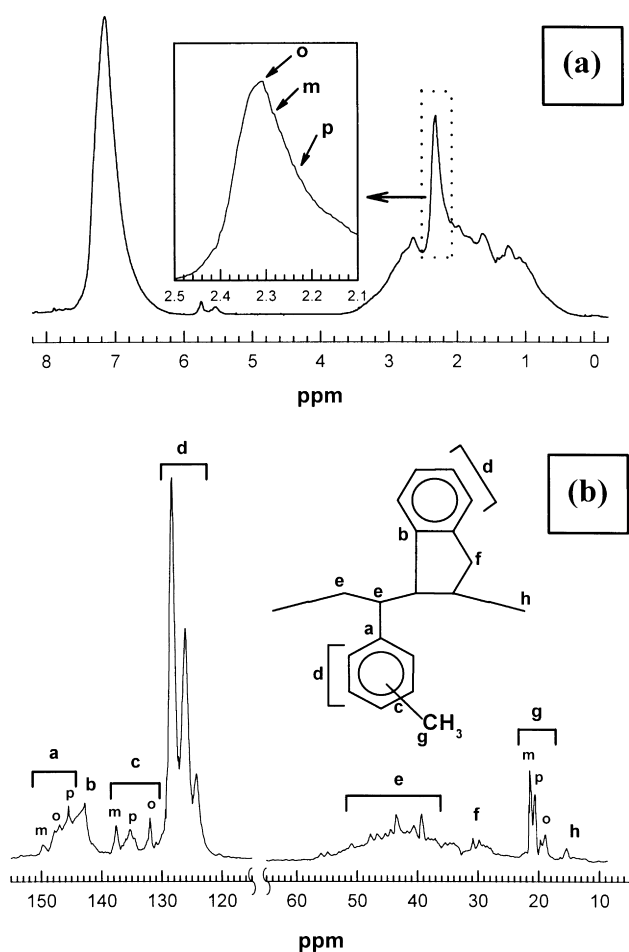


Fig. 1. ¹H (a) and ¹³C NMR (b) spectra for neat C-9 resin employed in this study.

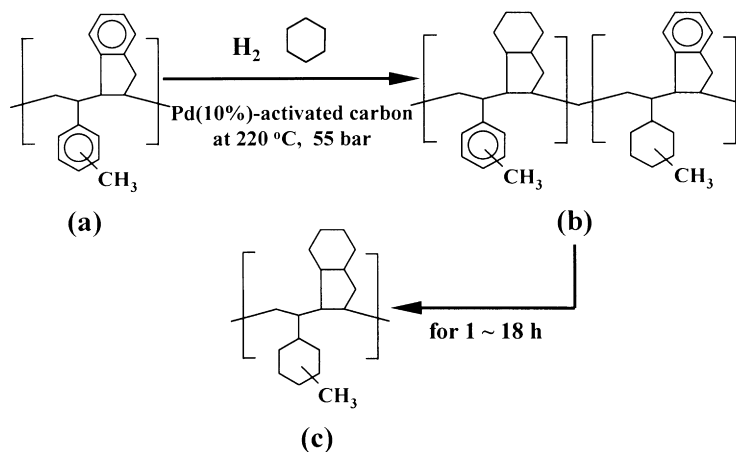


Fig. 2. Scheme describing the hydrogenation reaction: (a) neat C-9 resin; (b) partially hydrogenated C-9 resin; and (c) fully hydrogenated C-9 resin.

to 220°C at a rate 10°C/min. At this point, the reactor pressure was ca. 17 bar due to the high temperature. Then, the pressure inside the reactor was increased to 55 bar by adding hydrogen gas. When the hydrogenation reaction occurred, which reduced the pressure to 28 bar, the reactor pressure was again increased to 55 bar. The DH of C-9 resin was controlled by changing the amount of hydrogen and the reaction time between 1 h and 18 h. After the reaction, the reactor was cooled to room temperature with a cooling jacket, and the hydrogen gas inside the reactor was thoroughly vented with the aid of fresh nitrogen gas. The catalyst in the cyclohexane solution was removed using a cellite-filled glass filter. Finally, the solvent was completely removed in a fume hood for 7 days at room temperature and under a vacuum oven at 60°C for 2 days. The chemical structures of partially- and fully-hydrogenated C-9 resins are given in Fig. 2(b) and (c), respectively. We found that \bar{M}_w and \bar{M}_w/\bar{M}_n with increasing DH were not changed in GPC measurement. This is expected because the molecular weight increment was just 5%, even if neat C-9 resin was fully hydrogenated. Thus, we concluded that any chain scission and degradation did not occur during the reaction, even though the reaction condition employed in this study (220°C) was more severe than that reported in Refs. [22,23] where the reaction temperature was 140°C.

The DH of C-9 resins synthesized in this study was quantitatively determined by elemental analysis (EA, VareoEL). The chemical structures of C-9 resins were determined by Fourier transform infrared (FT-IR) spectroscopy (Bio-Red 375C) using the KBr disk method, ultraviolet/visible light spectroscopy (UV, Shimadzu) at a constant concentration 0.02 g of a resin per 100 g of cyclohexane. The T_g of hydrogenated C-9 resins was determined using differential scanning calorimetry (DSC, Perkin-Elmer 7 Series) at a heating rate of 10°C/min. The densities of the PSs and the C-9 resins with various DHs were measured using a density gradient column consisting of a methanol and ethylene glycol system at 26°C. The swelling

effect of the specimen in the mixed solvent was negligible, because of no change in the specimen height in the column for 24 h.

2.3. Turbidity measurement

Several compositions of each blend system, PB/C-9 resin and PS/C-9 resin systems with various DHs, were prepared by dissolving a predetermined amount of mixture into toluene (10 wt% in solid). The solvent was slowly evaporated at room temperature in a fume hood for 24 h and completely removed under vacuum at 60°C for 24 h. The specimen thickness was ca. 20 μm . The turbidity point (T_b) of the specimen was determined by light scattering using a He-Ne laser (5 mW) at a wavelength of 632.8 nm and a photomultiplier tube detector. T_b was determined by the temperature at which the scattering intensity at a scattering angle of 30° increased abruptly during cooling at a rate of 1.0°C/min from the homogeneous state (say 15–20°C above the T_b). For some blends, the cooling rate was varied from 1.0 to 0.1°C/min in order to obtain reproducibility of the T_b within $\pm 0.2^\circ\text{C}$.

3. Results and discussion

3.1. Characterization of HRs and the degree of hydrogenation

HRs with various values of DH ranging from 0 up to 0.951 were synthesized in this study, as listed in Table 2. The values of DH in Table 2 were determined by the EA of C and H atoms, since we found that the C-9 resin employed in this study was only composed of C and H by spectroscopic analysis. Hereafter, a hydrogenated C-9 resin with a certain value of DH will be denoted as HR-xyz resin, where xyz refers to the conversion of the aromatic rings to alicyclic rings divided by a thousand. Also, given in Table 2 are the

Table 2
The hydrogenated resins with various degrees of hydrogenation

Samples code	Mole ratio ^a (H/C)	Degree of hydrogenation ^b	Density ^c (g/cc)
Neat C-9 resin	1.050	0.0	1.0878
HR-056	1.085	0.056	1.0734
HR-162	1.152	0.162	1.0659
HR-298	1.238	0.298	1.0520
HR-385	1.293	0.385	1.0411
HR-488	1.358	0.488	1.0328
HR-667	1.471	0.667	1.0145
HR-699	1.491	0.699	1.0134
HR-759	1.529	0.759	1.0057
HR-846	1.584	0.846	0.9991
HR-873	1.601	0.873	0.9986
HR-900	1.618	0.900	0.9982
HR-914	1.627	0.914	0.9963
HR-940	1.643	0.940	0.9935
HR-951	1.650	0.951	0.9908

^a Determined by elemental analysis (EA).

^b Estimated from EA results.

^c Determined by a density gradient column measurement using methanol–ethylene glycol solution at 26°C.

densities of HRs, and variations of the density with DH are given in Fig. 3. It can be seen in Fig. 3 that the density (ρ) of HR decreases linearly with increasing DH:

$$\rho_{\text{HR-resin}} = 1.0811 - 0.09547\text{DH} \quad (1)$$

The decrease of density with increasing DH is attributed to the longer bond length of the cyclic single bonds compared to the aromatic double bonds. However, the density change is not due to a small increase of molecular weight with increasing DH. As mentioned above, the change of \bar{M}_w and \bar{M}_w/\bar{M}_n with increasing DH in all HRs synthesized was not detectable using GPC chromatograms. The results

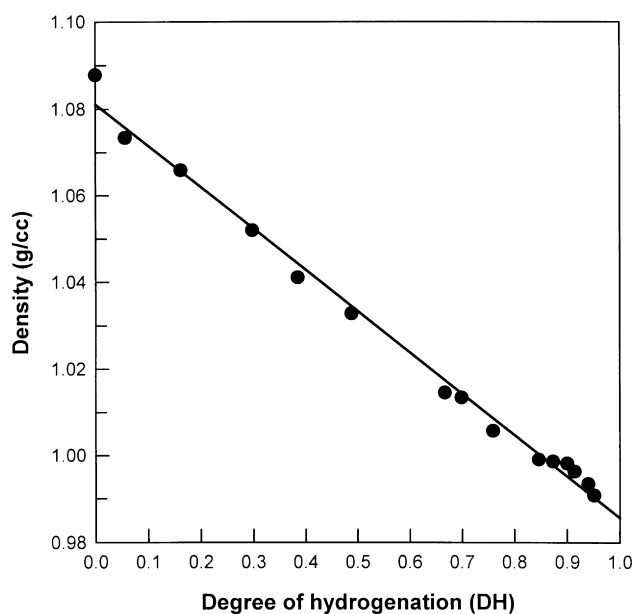


Fig. 3. Plots of density versus DH of C-9 resin synthesized in this study.

of density measurement are in good agreement with those of EA.

Fig. 4 gives the FT-IR spectra for various HRs. As DH increased, the aliphatic C–H stretching peaks at wave numbers (ν) of 2925 and 2853 cm^{-1} increased. Also, the aromatic C–H stretching peaks at ν of 3062 and 3025 cm^{-1} , the aromatic C=C stretching peaks at ν of 1603 and 1493 cm^{-1} , and the aromatic C–C out-of-bending peaks at ν of 750 and 701 cm^{-1} decreased with increasing DH. Here, the CH₃ bending peaks at ν of 1450 and 1375 cm^{-1} were used as the internal reference peaks. The observation that the aliphatic peak absorbance increases, while the aromatic peak absorbance decreases, with increasing DH is qualitatively consistent with the results given in Table 2.

Fig. 5 gives the UV spectra of various HRs. The maximum of the aromatic secondary peak at a wavelength (λ_{max}) of 266–280 nm decreases with increasing DH. Interestingly, however, the decrease in the peak height with increasing DH was not linear, rather the peak was shifted towards the higher wavelength (red shift) with increasing DH. For instance, λ_{max} of C-9 resin was 266 nm, but this was increased to 280 nm for HR-951. Due to a red shift in λ_{max} , the peak absorbance did not follow the Lambert–Beer relationship.

In order to explain the reason why a red shift occurred, ¹H NMR spectroscopy is employed and the results are given in Fig. 6. With increasing DH, the peak intensity at 7.2 ppm corresponding to the aromatic hydrogen decreased and the double bond peaks in a chain end appearing at 5.54 and 5.75 ppm disappeared. From the inset in Fig. 6, one notes that with increasing DH, two peaks at 2.32 and 2.29 ppm decrease significantly compared to the peak at 2.23 ppm, and only one peak at 2.23 ppm is observed for HR-951. This implies that the hydrogenation reaction started at the

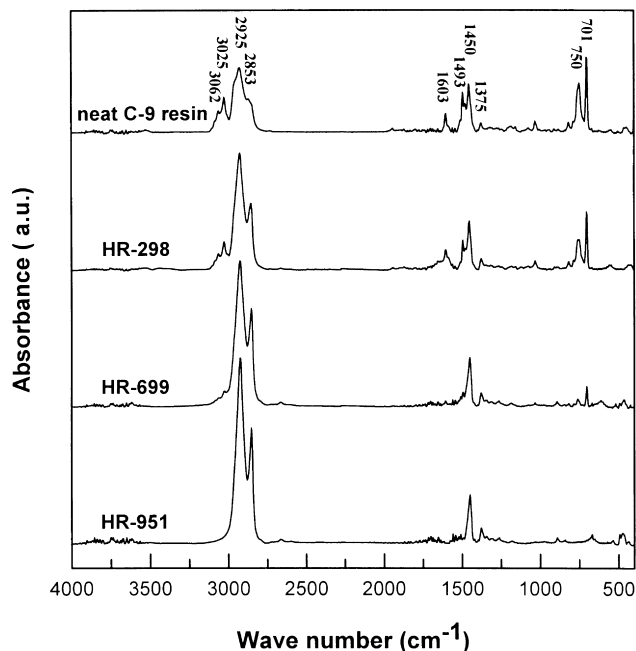


Fig. 4. FT-IR spectra for various HRs synthesized in this study.

ortho and *meta* isomers of vinyl toluene as well as the indene unit. When DH exceeded ca. 0.7, the hydrogenation reaction occurred at the isomer of vinyl toluene. This is due to the fact that the Pd catalyst employed in this study was more selective than the Ni catalyst. These results can now explain the red shift in the UV spectra with increasing DH (see Fig. 5), since the values of λ_{\max} of *ortho*, *meta* and *para* isomers of vinyl toluene are 263, 264 and 279 nm, respectively, and the λ_{\max} of an indene is 272 nm.

The values of T_g of C-9 resin and HR-951 resin are 58 and

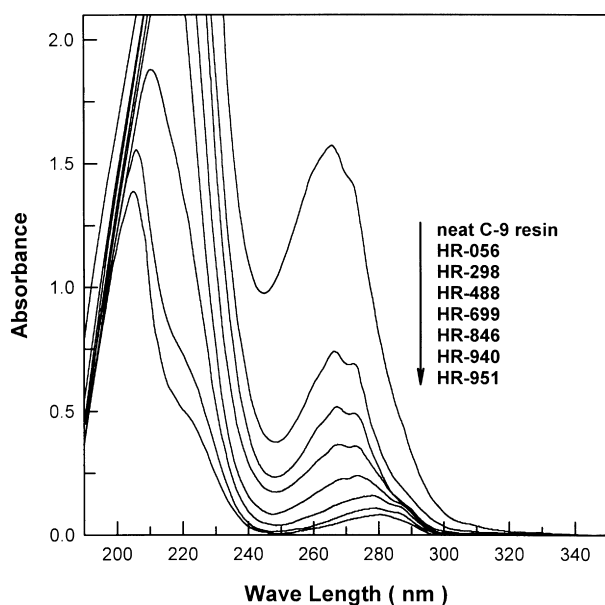


Fig. 5. UV spectra for various HRs synthesized in this study.

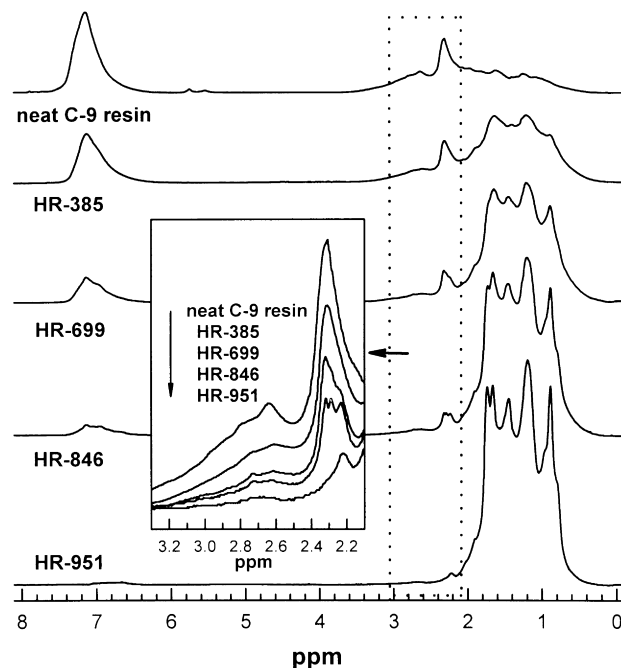


Fig. 6. ^1H NMR spectra for various HRs synthesized in this study.

66°C, respectively. During the first heating run, there is an additional melting peak near the T_g due to the lower molecular weight of C-9 resin and HRs. But, once C-9 resin and HRs were heated to 130°C followed by quenching, only T_g appeared during the second heating run. Previously, Gelsen and Bates [22,23] reported that when PS was fully hydrogenated to PVCH, the T_g of PVCH was ca. 40°C higher than that of PS. The small increment of T_g with increasing DH of C-9 resin might be attributed to the existence of an indene unit in the C-9 resin or relatively low molecular weight of HRs compared with high molecular weight of PS.

3.2. Phase behavior

The change in light scattering intensity, measured at a scattering angle of 30° with decreasing temperature for various blend compositions of PB/neat C-9 resin blend, is given in Fig. 7 and each curve is shifted vertically to avoid overlapping. T_b was taken as the intersection of the two slopes given in Fig. 7 (marked by the arrow). Fig. 8 gives phase diagrams for seven PB/HR pairs (neat C-9 resin, HR-056, HR-162, HR-873, HR-914, HR-940 and HR-951), showing that all blends exhibited upper critical solution temperature (UCST) above which a homogeneous mixture was obtained. Thus, with increasing temperature χ decreases, and a favorable interaction is enhanced. This is because there is no intermolecular interaction except for the van der Waals repulsive force between the constituent components. The solid curve for each blend system was theoretically predicted by the Flory–Huggins lattice model with the interaction energy density (α in mol/cc given by χ

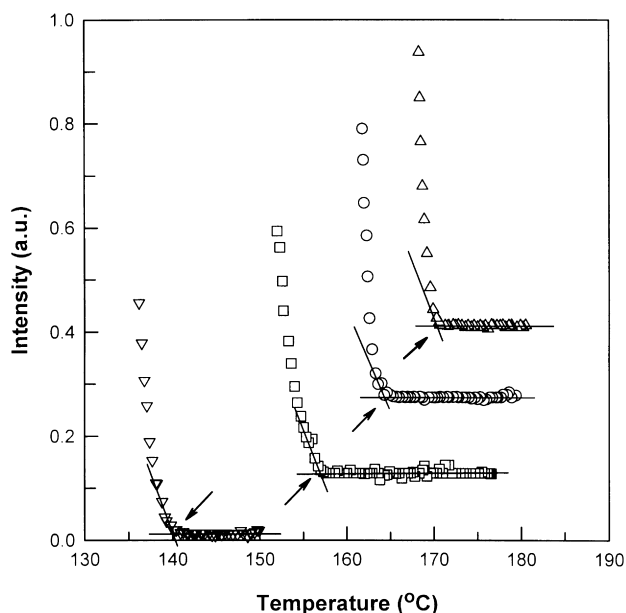


Fig. 7. Variations of light scattering intensity with temperature at 30° during the cooling scan at a rate of $1^\circ\text{C}/\text{min}$ for four different compositions of PB/C-9 resin blend. The weight fraction of PB in the blend is: (O) 0.03; (Δ) 0.1; (\square) 0.2; and (∇) 0.3. Three curves are arbitrarily shifted to avoid overlapping.

divided by V_{ref} where V_{ref} is the reference monomer volume) [21,24]:

$$\alpha = a + (b + c\phi_i)/T; \quad i = \text{PB or PS} \quad (2)$$

where ϕ_i is the volume fraction of PB (or PS) in the blend and T is the absolute temperature. In calculating the binodal curve, the specific volume (v_{sp}) of PB is taken as $1.1352 \text{ cm}^3/\text{g}$ and the v_{sp} of PS is taken as $0.9540 \text{ cm}^3/\text{g}$, measured using the density gradient column at 26°C .¹ The v_{sp} of HR with various DHs is equal to the inverse of the density given in Table 2.

The values of a , b and c in Eq. (2), determined for the PB/HRs blend, are given in Table 3, showing that with increasing DH, the value of b decreases for PB/HRs blend with $\text{DH} < 0.2$, whereas it increases for PB/HRs blends with $\text{DH} > 0.85$. Further, with increasing DH, the value of α at a given volume fraction of PB in the blend and turbidity temperature decreases for $\text{DH} < 0.2$, while it increases for $\text{DH} > 0.85$. Thus, a minimum value of α (i.e. the most favorable interaction between PB and HRs) at a given volume fraction of PB in the blend and turbidity temperature exists for the blends with $\text{DH} = 0.2 - 0.85$. It should be noted that the values of c in Eq. (2) are not negligible for all PB/HRs blends investigated. If the concentration dependent term (c) in Eq. (2) is neglected, the critical

¹ The specific volumes of PB [24] and PS [25] depended upon temperatures. However, in this study, the constant values are used for the specific volumes of PB and PS. This is because we did not measure the density variation with temperature for all HR resins.

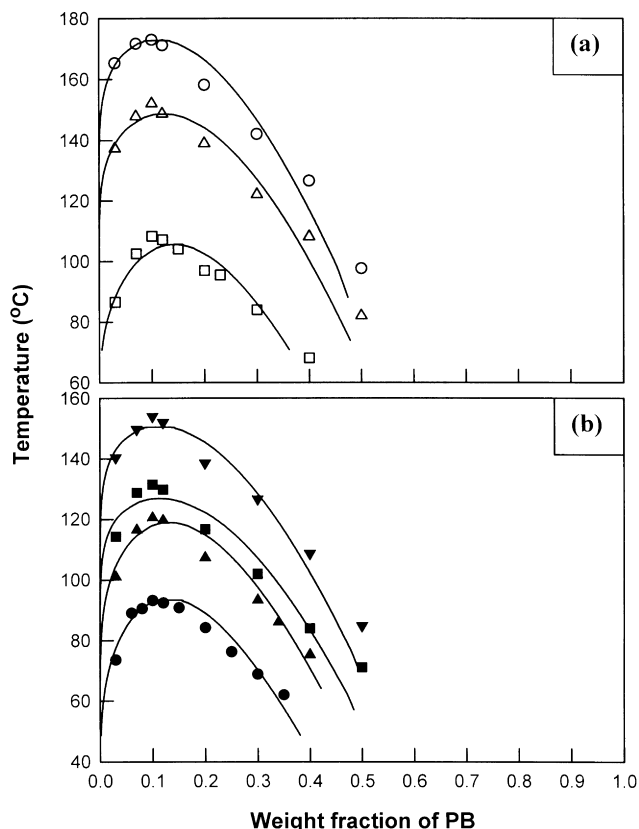


Fig. 8. (a) Phase diagrams for: (O) PB/neat C-9 resin, (Δ) PB/HR-056, and (\square) PB/HR-162. (b) Phase diagrams for: (\bullet) PB/HR-873, (\blacktriangle) PB/HR-914, (\blacksquare) PB/HR-940, and (\blacktriangledown) PB/HR-951. The solid curve for each blend system is a binodal curve calculated from the Flory–Huggins theory with the expressions of α given in Table 3.

volume fraction of PB (ϕ_c) in the blend is given by the Flory–Huggins theory:

$$\phi_c = 1/(1 + \sqrt{V_{\text{PB}}/V_{\text{HR}}}) \quad (3)$$

in which V_{PB} and V_{HR} are the molar volumes of PB and HR, respectively. When Eq. (3) is employed, the predicted value of ϕ_c for PB/HR blends is 0.035, which is considerably smaller than 0.1 determined experimentally. The predicted binodal curves are consistent with experimental turbidity curves.

Fig. 9 gives variations of UCST with DH for PB/HR blends. When the DH in HR is lower than approximately 0.2, UCST decreases with increasing DH, implying that the miscibility of PB/HR blends was enhanced. This is because a favorable interaction between the PB and the aromatic unit is worse than that between the PB and the alicyclic unit. However, when the DH in HR was greater than approximately 0.85, the blend became turbid at room temperature. Further, the UCST of this blend *increases* with increasing DH for $\text{DH} > 0.85$, which is the highlight of this paper. The above observations lead us to conclude that the miscibility of PB/HR blends is *not* always enhanced with increasing

Table 3
Interaction parameters determined by turbidity measurement

Blend systems	UCST (°C)	Interaction parameter (α) (mol/cc)
PB/neat C-9 resin	173	$\alpha = 0.3955 \times 10^{-3} + (0.1665 + 0.1012\phi_{PB})/T$
PB/HR-056	152	$\alpha = 0.3993 \times 10^{-3} + (0.1538 + 0.0982\phi_{PB})/T$
PB/HR-162	108	$\alpha = 0.4741 \times 10^{-3} + (0.1109 + 0.0934\phi_{PB})/T$
PB/HR-873	93	$\alpha = 0.4581 \times 10^{-3} + (0.925 + 0.0790\phi_{PB})/T$
PB/HR-914	121	$\alpha = 0.4289 \times 10^{-3} + (0.1099 + 0.0846\phi_{PB})/T$
PB/HR-940	132	$\alpha = 0.3344 \times 10^{-3} + (0.1458 + 0.0806\phi_{PB})/T$
PB/HR-951	154	$\alpha = 0.3492 \times 10^{-3} + (0.1471 + 0.0847\phi_{PB})/T$
PS-200/HR-488	123	$\alpha = 0.0254 \times 10^{-3} + (0.2919 + 0.1042\phi_{PS})/T$
PS-200/HR-667	179	$\alpha = -0.3893 \times 10^{-3} + (0.5128 + 0.1083\phi_{PS})/T$
PS-200/HR-699	224	$\alpha = -0.4003 \times 10^{-3} + (0.5689 + 0.1269\phi_{PS})/T$
PS-200/HR-759	262	$\alpha = -0.3978 \times 10^{-3} + (0.6028 + 0.1376\phi_{PS})/T$
PS-8/HR-759	136	$\alpha = -0.2467 \times 10^{-2} + (1.3822 + 0.1905\phi_{PS})/T$
PS-8/HR-846	175	$\alpha = -0.2793 \times 10^{-2} + (1.6658 + 0.2060\phi_{PS})/T$
PS-8/HR-900	182	$\alpha = -0.2860 \times 10^{-2} + (1.7272 + 0.2093\phi_{PS})/T$
PS-8/HR-951	233	$\alpha = -0.3243 \times 10^{-2} + (2.1023 + 0.2269\phi_{PS})/T$

DH. Although the exact reason for this behavior is not clear, it might be attributable to the fact that the HR employed in this study are random copolymers consisting of vinyl toluene, indene and their hydrogenated units. Therefore, in order to understand in detail this interesting UCST behavior, one must investigate the effect of DH on the miscibility (or UCST) of a blend system consisting of PB and an oligomeric vinyl toluene, and a blend system consisting of PB and an oligomeric indene.

Of particular noteworthy in Fig. 9 is a decrease of UCST with increasing DH. This is smaller at lower values of DH, compared to the increase in UCST at higher values of DH. The blends with DH ranging from 0.3 to 0.85 were transparent; thus we could not detect the turbid points by the light scattering method. Even in this situation, we speculate that the most favorable interaction might be expected for the blend with DH of approximately 0.7 which was obtained by the extrapolation of two UCST curves located at lower and higher values of DH in Fig. 9.

Fig. 10(a) shows the phase diagrams for four pairs of PS-8/HR blends (HR-759, HR-846, HR-900 and HR-951) and Fig. 10(b) gives another four pairs of PS-200/HR blends (HR-488, HR-667, HR-699 and HR-759). The solid curve for each blend system was theoretically predicted by the Flory–Huggins lattice model with the interaction intensity density (α in mol/cm³) using Eq. (2). The values of a , b and c for the blend systems are given in Table 3. The value of b increases steadily with increasing DH for the PS-200/HR blends as well as the PS-8/HR blends. Further, with increasing DH, the value of α increases at a given volume fraction of PS in the blend and temperature. In this study, we could only detect the range of T_b between 110 and 270°C, because the T_g of PS is about 100°C and degradation of the resin may occur at temperatures above 270°C. In Fig. 10(a) and (b) it is observed that all blends exhibit UCST and the critical weight fraction of PS (w_c) does not change with DH. Also, we observe $w_c \approx 0.18$ for PS-200/HR blends, which

is smaller than $w_c \approx 0.4$ for PS-8/HR blends. This is due to the smaller molecular weight of PS in the PS-8/HR blends, which is expected from the Flory–Huggins theory. However, the values of a , b and c for PS-200/HR-759 blend are different from those for PS-8/HR-759. If the Flory–Huggins theory with α given by Eq. (2) holds for these blend systems, the values of a , b and c for the two blends should be the same. However, when the expression for α determined from the PS-200/HR-759 blend is employed to predict the UCST of the PS-8/HR-759 blend, the predicted value is 174°C, which is about 40°C higher than the experimental value of 136°C. Thus, the above result implies that α in Eq. (2) should be a function of the molecular weight of PS. This behavior is consistent with the

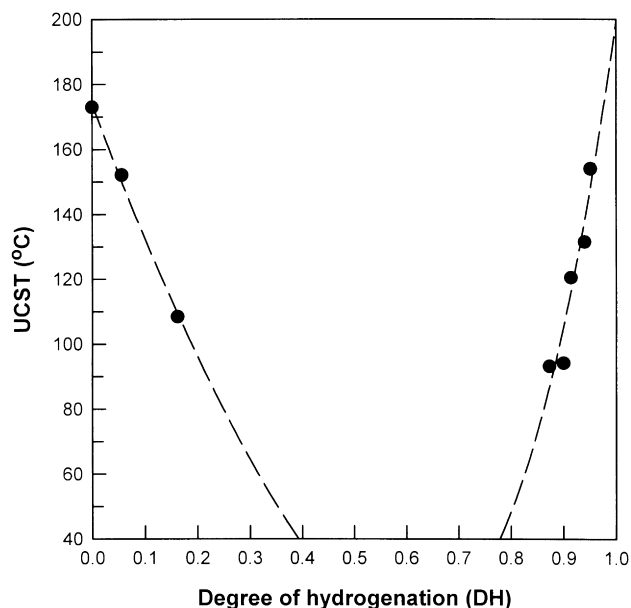


Fig. 9. Variations of UCST with DH of C-9 resin in PB/HR resin blends. The dashed lines are drawn to guide the eyes.

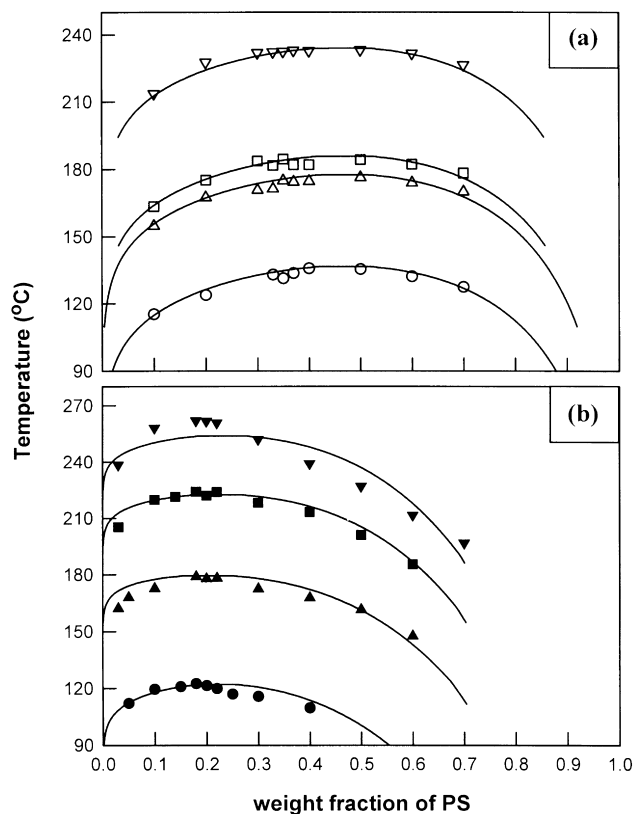


Fig. 10. (a) Phase diagrams for: (○) PS-8/HR-759, (△) PS-8/HR-846, (□) PS-8/HR-900, and (▽) PS-8/HR-951. (b) Phase diagrams for: (●) PS-200/HR-488, (▲) PS-200/HR-667, (■) PS-200/HR-699, and (▼) PS-200/HR-759. The solid curves for each blend system are binodal curves calculated from the Flory–Huggins theory with the expressions of α given in Table 3.

results reported by Han et al. [21]. They found that when 1,2-addition in the PEB is 84 wt%, the expression for α determined from PS-N1/PEB-84L blends (the \bar{M}_w of the PEB = 1465) is different from that determined from PS-N1/PEB-84H blends (the \bar{M}_w of the PEB = 3629). They also showed that the T_{ODT} of polystyrene-*block*-poly(ethylene-*co*-butene-1) copolymer predicted by the α determined for the latter is higher than that predicted by the α determined from the former. (See Fig. 14 in Ref. [21]).

Fig. 11 describes the dependence of UCST on DH for PS/HR blends, showing that UCST increases with increasing DH. Although the most favorable interaction between PS and HR should occur at a certain value of DH between 0 and 0.4 by means of the solubility parameter approach, we could not unambiguously determine the DH corresponding to the most favorable interaction because the blends do not exhibit any turbidity. Further, it was found that even if a PS having the molecular weight of 4×10^6 was blended with HR, these were transparent whenever DH in HR was lower than 0.4.

3.3. Analysis of miscibility data using the solubility parameter

The results that the most favorable interaction of the

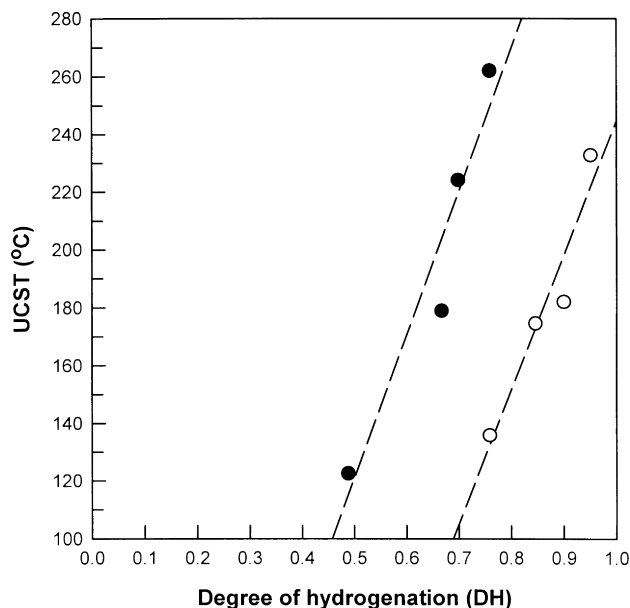


Fig. 11. Variations of UCST with DH of C-9 resin in PS-8/HR blends (○) and PS-200/HR blends (●). The dashed lines are drawn to guide the eyes.

PB/HR blends system is expected at $DH \approx 0.7$ (see Figs. 8 and 9) can be qualitatively explained by the solubility parameter (δ). Although in the literature different values of δ are reported for a given component, in this study we chose the values of δ in Ref. [26]. When the values of δ for some components were not available in Ref. [26], they were estimated using Hoy's group contribution method [27]. The effect of microstructure (1,2-addition and *cis*-1,4-addition, *trans*-1,4-addition in PB, *ortho*, *meta* and *para* isomers of vinyl toluene) on the estimation of δ was also considered. Using the values (unit: $(J/cm^3)^{1/2}$) of $\delta = 17.27$ for 1,2-PB, $\delta = 18.27$ for *trans*-1,4-PB, $\delta = 18.51$ for *cis*-1,4-PB, $\delta = 19.30$ for the *ortho* isomer, $\delta = 19.24$ for the *meta* isomer, and $\delta = 19.86$ for the *para* isomer of vinyl toluene, $\delta = 20.48$ for indene, $\delta = 17.31$ for fully hydrogenated vinyl toluene, and $\delta = 18.35$ for fully hydrogenated indene, we estimate: $\delta = 18.29$ for PB, $\delta = 19.96$ for neat C-9 resin, and $\delta = 17.85$ for HR-1000, respectively. When the value of δ for HR resin with a specific value of DH is estimated from the volume average of the δ values of neat C-9 resin and HR-1000, the δ of HR-780 becomes identical to that of PB, namely, the most favorable interaction is obtained at HR-780. Although this value (0.78) of DH is slightly different from the optimum value of DH (ca. 0.7), this result is consistent with the phase behavior given in Figs. 8 and 9.

Also, the solubility parameter for HR-290 was found to be identical to that of PS since the value of δ for PS was taken to be $19.35 (J/cm^3)^{1/2}$ [26]. But, we could not verify this argument since PS/HR blends did not exhibit any turbidity for $DH < ca. 0.4$. However, for $DH > 0.3$, the difference in δ between PS and HRs becomes greater with increasing DH. In other words, a favorable interaction

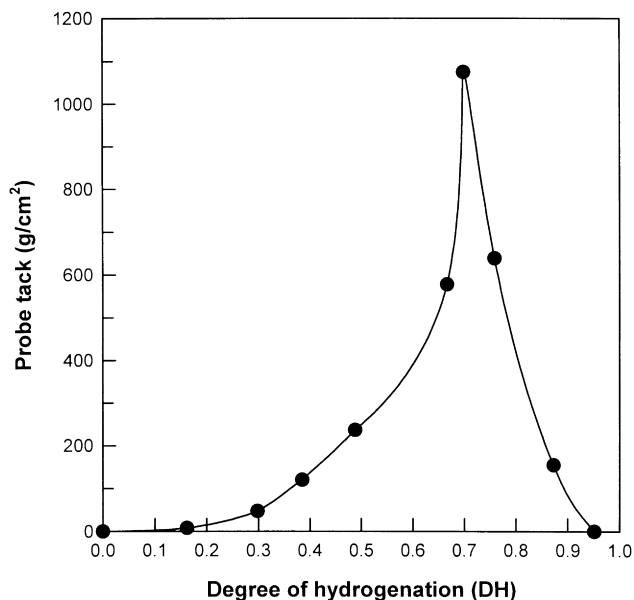


Fig. 12. Effect of DH of C-9 resin on probe tack for 60/40 (w/w) Kraton D1102/HR resin mixtures.

between PS and HRs decreases with increasing DH for $DH > 0.3$. This is qualitatively consistent with the phase behavior given in Fig. 10.

3.4. Tack properties of the mixtures of SBS triblock copolymer and HRs

On the basis of Fig. 9, it is reasonable to expect that at a given blend composition of PB/HR blends, the most favorable interaction between these components would occur for $DH \approx 0.7$. Since no turbidity was observed for the PB/HR blends with $DH = 0.2 - 0.8$, we tested indirectly the miscibility of the blends by measuring the tack properties of the mixtures of SBS triblock copolymer and HRs. The SBS triblock copolymer employed in this study is Kraton D1102 (Shell Development Co.) having block molecular weights of 9,000 PS-45,000 PB-9,000 PS [28]. The microstructures of the PB block (the mole percent of 1,2-addition, *trans*-1,4- and *cis*-1,4-additions in the PB block are 9.9, 42.9 and 47.2, respectively, as determined by ¹H NMR) of Kraton D1102 are almost the same as those in the PB employed in this study (see Table 1). Because the molecular weight of the PS block of Kraton D1102 is 9,000, we speculate from Fig. 11 that a favorable interaction between the PS block of Kraton D1102 and HRs would steadily decrease with increasing DH, especially for larger values of DH. Thus, the miscibility (or a favorable interaction) between the PB block of Kraton D1102 and HR would play an important role in determining the tack properties of Kraton D1102/HRs mixtures.

Among the many methods available for tack property measurement, we employed the probe tack test (ASTM D2979), which is regarded as being one of the most reliable

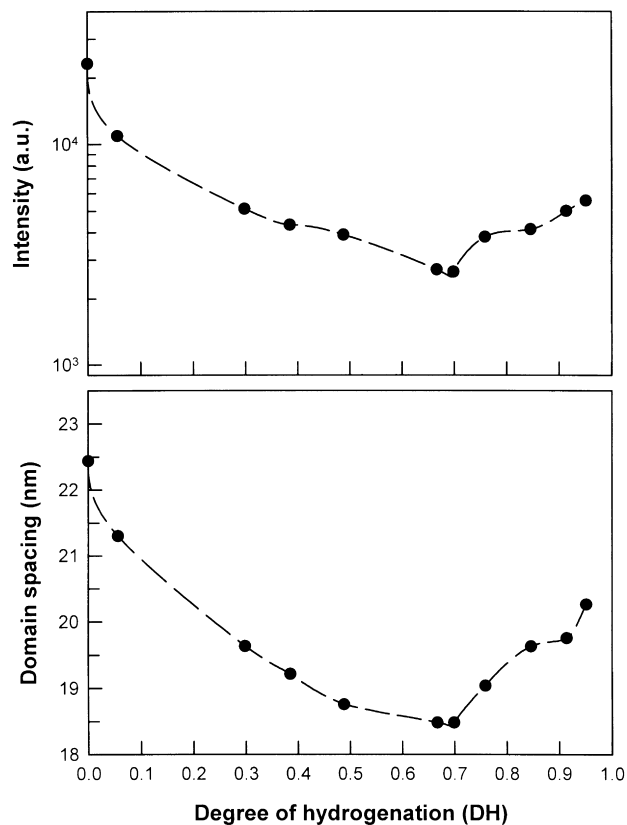


Fig. 13. (a) Plots of the first order peak of SAXS intensity versus DH of C-9 resin; and (b) interdomain spacing versus DH of C-9 resin for 50/50 (w/w) Kraton D1102/HR resin mixtures.

methods. Although the detailed experimental procedure is introduced elsewhere [29], we describe this method very briefly. An adhesive layer of 60/40 (w/w) Kraton D1102/HRs mixture, which exhibited maximum tack among all blend compositions, was prepared by solution coating (50% solid in toluene) onto a poly(ethylene terephthalate) backing film having the thickness of 52 μm , followed by the removal of the solvent using a convection oven at 100°C for 5 min. The complete removal of the solvent was done in a fume hood at room temperature for 5 days. After the probe was in contact with the adhesive layer for 1 s under a loading of 100 g/cm^2 , the probe tack was determined as the force in g/cm^2 required to separate the probe from the adhesive layer having the thickness of 0.15 mm. The cross-head speed of the probe was 10 mm/s. The probe surface was No. 304 stainless steel and the diameter of the probe was 5 mm (TE6002, Sangyo Co.).

The variations of probe tack with DH for 60/40 Kraton D1102/HR mixtures are given in Fig. 12, showing that the blends with DH less than 0.2 and greater than 0.9 do not exhibit any measurable tack, and that the blends with DH between 0.67 and 0.76 exhibit good tack properties. This observation can now be explained by Figs. 9 and 11, which show only a limited miscibility between PB block and HR resin for $DH < \text{ca. } 0.2$ and $DH > \text{ca. } 0.85$. It should be

mentioned that the 50/50 (w/w) Kraton D1102/HR mixture looked turbid for $DH > 0.91$, thus macrophase separation occurred and the dispersed phase of HR-951 was ca. $3 \mu\text{m}$ [29]. These results indicate that even though no macrophase separation between the components occurred, the blend did not exhibit any measurable tack unless a favorable interaction between PB and HR is observed. These results further suggest that as a favorable interaction between the PB block of Kraton D1102 and HR is increased, the tack property of Kraton D1102/HR mixtures increases. Therefore, the reason why the Kraton D1102/HR-699 mixture exhibits the highest tack property among all compositions tested is due to the most favorable interaction between PB block and HR. This conclusion is consistent with the results given in Fig. 9.

Fig. 13 gives plots of scattering intensity of the first order peak and the interdomain spacing, which is determined from $2\pi/q^*$ with q^* being the first-order peak position, versus DH for 50/50 (w/w) Kraton D1102/HR blends. These plots were obtained by synchrotron small-angle X-ray (SAXS) with 3C2 beam line at PLS, Korea. The details of the experimental procedures employed are described elsewhere [30,31]. It can be seen in Fig. 13 that a minimum intensity of the first-order peak and a minimum domain spacing occur for Kraton D1102/HR-699 mixture with $DH \approx 0.7$. A minimum domain spacing is expected for a blend with the most favorable interaction between PB block and HR. This observation is consistent with the results given in Fig. 12. Further, the results given in Figs. 12 and 13 are consistent with the observations made above in reference to Fig. 9: the most favorable interaction between PB and HR occurs for $DH \approx 0.7$.

4. Conclusions

We have shown that the degree of hydrogenation (DH) of an aromatic C-9 hydrocarbon resin was successfully controlled by monitoring the amount of hydrogen added and the duration of reaction. From turbidity measurement we have observed that a favorable interaction between HR and PS decreases with increasing DH . Very interestingly, however, a favorable interaction between HR and PB does not always be enhanced with increasing DH . There exists an optimum value of DH (ca. 0.7) which gives the most favorable interaction between HR and PB. These results are also interpreted with the aid of the solubility parameter (δ) determined from the group contribution method. We have shown that there exists a correlation between the miscibility of PB block with HR and the tack property, namely, as a favorable interaction between PB block and HR in Kraton D1102/HR mixture is increased, the tack property increases. This correlation is further supported by the dependence of the first-order peak of SAXS intensity and the domain spacing on the DH in HR. We conclude that the miscibility between the PB block of Kraton D1102 and HR plays an important role in

determining the tack property of Kraton D1102/HR mixtures.

Acknowledgements

We thank Dr M.S. Jeon at LG Chemical Company who supplied us with PB, and Dr I.K. Sung at Kolon Petrochemical Company who supplied us with C-9 resin. We also acknowledge that Hansol Company kindly allowed us to use a probe tack tester. This work was supported by Advanced Materials Programs (1998-017-E00026) administered by the Korea Research Foundation, Korea. Synchrotron SAXS experiment at 3C2 and 1B2 beam lines of the PLS was supported by the Ministry of Science and Technology (MOST) and Pohang Iron & Steel Company (POSCO).

References

- [1] Donatas S, editor. Handbook of pressure-sensitive adhesive technology New York: Wiley, 1982. pp. 353.
- [2] Aubrey DW, Sherriff M. J Polym Sci: Polym Chem Ed 1978;16:2631.
- [3] Sherriff M, Knibbs RW, Langley PG. J Appl Polym Sci 1973;17:3423.
- [4] Aubrey DW, Sherriff M. J Polym Sci: Polym Chem Ed 1980;18:2597.
- [5] Kraus G, Jones FB, Marrs OL, Rollmann KW. J Adhes 1977;8:235.
- [6] Kraus G, Rollmann KW. J Appl Polym Sci 1977;21:3311.
- [7] Kraus G, Rollmann KW, Gray RA. J Adhes 1979;10:221.
- [8] Kraus G, Hashimoto T. J Appl Polym Sci 1982;27:1745.
- [9] Class JB, Chu SG. J Appl Polym Sci 1985;30:805 (see also pages 815 and 825).
- [10] Fox TG. Bull Am Phys Soc 1956;1:123.
- [11] Kim J, Han CD. J Polym Sci Part B: Polym Phys 1988;26:677.
- [12] Han CD, Kim J, Baek DM. J Adhes 1989;28:201.
- [13] Han CD, Kim J, Baek DM. J Polym Sci: Polym Phys Ed 1990;28:315.
- [14] Dahlquist CA. In: Patrick RL, editor. Treatise on adhesion and adhesives, New York: Marcel Dekker, 1969. pp. 219.
- [15] Toig BW, Mancinelli PA. Elastomerics 1990;122(10):44.
- [16] Fetters LJ, Lohse DJ, Richter D, Witten TA, Zirkel A. Macromolecules 1994;27:4639.
- [17] Ferry JF. Viscoelastic properties of polymers, 3. New York: Wiley, 1980.
- [18] Kawahara S, Akiyama S. Polymer 1991;32:1681.
- [19] Kawahara S, Kano Y, Akiyama S. Int J Adhes and Adhesives 1993;13:181.
- [20] Kawahara S, Akiyama S. Macromolecules 1993;26:2428.
- [21] Han CD, Chun SB, Hahn SH, Harper SQ, Savickas PJ, Meunier DM, Li L, Yalcin T. Macromolecules 1998;31:394.
- [22] Gehlsen MD, Bates FS. Macromolecules 1993;26:3611.
- [23] Gehlsen MD, Bates FS. Macromolecules 1993;26:4122.
- [24] Rigby D, Roe RJ. Macromolecules 1986;19:721.
- [25] Richardson MJ, Savill NG. Polymer 1977;18:3.
- [26] Van Krevelen DW. Properties of polymers, 3rd. New York: Elsevier, 1990.
- [27] Hoy KL. J Coated Fabrics 1989;19:53.
- [28] Ryu DY, Kim JK. Polymer. Submitted for publication.
- [29] Ryu DY. The miscibility and tack properties of the mixtures of hydrogenated C-9 resin and block copolymers, MS Thesis, Pohang University of Science and Technology, Pohang, Korea, 1999.
- [30] Park BJ, Rah SY, Park Y, Lee KB. Rev Sci Instrum 1995;66:1722.
- [31] Kim JK, Lee HH, Ree M, Lee KB, Park Y. Macromol Chem Phys 1998;199:641.